DESIGN INSTRUMENTATION AND PERFORMANCE OF A GEOGRID REINFORCED TEST FILL

by

Y. Liu[1], J.D. Scott[1], D.C. Sego[1] and V. Diyaljee[2]

ABSTRACT

A 12 m high instrumented cohesive soil test embankment with 45° slopes reinforced with geogrids has been built near Devon, Alberta. The embankment has four instrumented slopes: three slopes reinforced with different types of geogrids and one unreinforced. Details of the design, construction and instrumentation of the test fill are described. Field measurements from the Tensar geogrid reinforced section, during the three years of construction and two years after completion of the fill, are outlined and discussed.

Keywords: construction, geogrid, instrumentation, field measurements

[1] Department of Civil Engineering, University of Alberta, Edmonton, AB, T6G 2G7

[2] Geotechnical Services Section, Material Engineering Branch, Alberta Transportation and Utilities, 4999 - 98 Avenue, Edmonton, AB, T6B 2X3

INTRODUCTION

Geotextiles and geogrids have been used extensively as soil reinforcing members in geotechnical engineering design and construction for steep slopes and retaining walls. The use of reinforcement reduces the cost of construction and makes some engineering projects possible which would be difficult using conventional construction methods.

Reinforced slopes are designed mainly using limit equilibrium methods. Limit equilibrium analysis for reinforced slopes (Murray, 1982, Jewell et al., 1984, Duncan et al., 1985, Schmertmann et al., 1987) is based on conventional slope stability analysis methods. The reinforcing members are incorporated into the analysis either as a free body resisting force (or moment), or by improving the soil shear strength. To properly use limit equilibrium analysis, one needs to understand the mechanism and failure modes of reinforced slopes and to evaluate the mobilization of the strengths and the strain compatibility of the soil and the reinforcing members.

When deformation of a reinforced slope is of concern, limit equilibrium methods cannot provide satisfactory predictions. To overcome the disadvantages of limit equilibrium methods, finite element methods have been introduced to analyze the stress and strain distributions within the reinforced slopes (Rowe, 1984, Chalaturnyk, 1988). However, in finite element modelling of the soil, the reinforcement and, more important, the interaction between the soil and the reinforcement must be incorporated into the finite element program for use in engineering practice. Therefore, instrumented full scale tests of reinforced slopes become necessary for developing and using limit equilibrium and finite element methods to compare predictions to actual performance.

Several instrumented full scale slopes for research purposes are reported in the literature, for example, Fannin and Hermann (1988), Bassett and Yeo (1988), Rimoldi (1988). In the majority of cases geogrids have been used to reinforce granular materials. In order to obtain a better understanding of reinforcement mechanism in cohesive soils and accumulate experience for both analytical and design purposes, the Geotechnical Section, Material Engineering Branch, and the Research and Development Branch of Alberta Transportation and Utilities, together with the Department of Civil Engineering, University of Alberta, have cooperated to carry out a research project on a reinforced embankment constructed of cohesive soil.

The test embankment was built near Devon, Alberta, approximately 30 km from Edmonton (Fig. 1) (Sego et al., 1990). It was constructed to a design height of 12 m in three stages from 1986 to 1988. The test fill has four slope sections, three are reinforced with different types of geogrids, namely Tensar, Signode and Paragrid, and the fourth slope is unreinforced for comparison (Fig. 2). A large number of monitoring instruments were installed in the fill and readings were taken at specified intervals so that the performance of the test fill during and after construction could be monitored.

In this paper, the objectives and design considerations of the test fill are first described. Details of the soil properties in the fill and the foundation are presented along with a description of the fill construction and the instrumentation installed in the fill. Field measurements showing the performance of the test fill are then discussed. Due to the limitation on the paper's length, only the performance of the Tensar geogrid reinforced section is presented.

OBJECTIVES AND DESIGN CONSIDERATIONS OF THE TEST FILL

The primary objective of the test fill was to determine how individual geogrid layers reinforce a mass of cohesive soil. The understanding of the reinforcement mechanism should lead to a better understanding of the most critical modes of failure and result in a more efficient and economical design method for slope reinforcement. Additional objectives were to evaluate the current methods used to design fills using geogrids as reinforcement, to compare the performance of three different

geogrid materials, to evaluate the field performance of the compacted fill and its foundation soils, and to evaluate the procedures used to construct geogrid reinforced slopes.

The high strength and high modulus geogrids used in the test fill can modify the magnitude and distribution of the lateral deformation and thus the stress distribution in the embankment. One major purpose of the research was to measure the stress transfer from the soil to the geogrids during the construction of the embankment. The test slopes were designed with a low factor of safety to develop lateral strain in the soil which would mobilize the tensile strength of the geogrids. To ensure that lateral strains would occur and to ensure that each reinforcing layer would act independently, only three primary reinforcing layers at a 2 m vertical spacing were installed in the test fill (Fig. 3). This low number of geogrid layers was chosen to increase the efficiency so that both local and overall stability of the slope was achieved while allowing for soil deformation to occur.

PROPERTIES OF SOILS

The grain size curve of the fill material is given in Figure 4. The soil is composed of 25% sand, 50% silt and 25% clay sizes. Although this material would be described as a clayey silt on the basis of the grain size curve, the Atterberg limits are indicative of an inorganic clay of low to medium plasticity. The liquid limit of the fill soil is 42% and the plastic limit is 18%. The activity of the soil is therefore, approximately equal to one. X-ray diffraction tests show that the clay fraction is largely montmorillonite.

Standard compaction tests were conducted on the fill soil, (Hofmann, 1989). The resulting compaction curve is shown in Figure 5, where the optimum water content is approximately 21.5% and the corresponding maximum dry density is 1,600 kg/m^3. The undrained shear strength of the compacted soil drops rapidly at water contents above the optimum (Fig. 5). Compaction criterion for placement water content for the test fill was specified at 22% to 24%, since the stress-strain curves obtained from the unconfined compression tests at this moisture content indicated a significant deformation prior to failure. Such deformation was required to mobilize the tensile force in the reinforcement members. Also, at water content between 22% to 24%, the fill soil was estimated to have an undrained shear strength of about 50 kPa which yields a design factor of safety of between 1.0 to 1.2 for a 12 m high unreinforced embankment with 1:1 side slopes.

Shelby tube samples were taken from the test fill and unconsolidated undrained triaxial shear tests were conducted under confining pressure of 0, 80, 160, 240 and 360 kPa, (Hofmann, 1989). The undrained shear strength of 76.3 kPa at no confining pressure, increased slightly with confining pressure because the average degree of saturation of the fill soil was 92%. Unconsolidated undrained triaxial shear tests were also carried out, under confining pressure of 0, 80, 160 and 240 kPa, on laboratory compacted samples saturated with a back pressure. An average undrained shear strength of 76 kPa was obtained.

Consolidated undrained triaxial shear tests with pore pressure measurements were also conducted on the compacted fill soil (Fig. 6), (Hofmann, 1989). The soil was compacted in a standard compaction mould at water contents between 22% and 24%. Specimens were then removed from the mould using thin walled, 38 mm diameter Shelby tubes. The specimens were consolidated under confining pressures of 75, 150, 200 and 300 kPa prior to shearing. Typically, the soil exhibited strain strengthening behavior, where the deviatoric stress had not yet reached a maximum at 18% strain. It, therefore, became necessary to define failure in terms of the maximum principal effective stress ratio reached during shearing of the specimens. In most cases, the principal effective stress ratio reached a maximum of 3.0 at axial strains of about 12%. The pore pressures, however, rapidly increased, reaching a maximum at 4% strain. The pore pressure parameter A was equal to approximately 0.50 for high confining stresses and equal to about 0.16

for low confining stresses. The tests gave an effective friction angle of 22 degrees and an effective cohesion of 13 kPa.

The test fill was founded on glaciolacustrine sediments. A number of boreholes were drilled in the foundation soils to a depth of 10 m with a wet rotary drill rig (Hofmann, 1989). Standard penetration tests and Shelby tube samples were taken alternately. A typical profile is shown in Figure 7. The uppermost layer of soil consists of a soft silty clay at a water content of 35%. This is underlain by 2 m of a stiffer sandy, silty clay. Beyond 6 m, a fine, very dense layer of grey sand exists and this is underlain by a hard clay till. Consolidation tests have shown that the effective preconsolidation stress in the soft silty clay is approximately 350 kPa.

Consolidated undrained triaxial shear tests with pore pressure measurements were conducted on Shelby tube samples and block samples of the soft silty clay foundation soil, (Hofmann, 1989). Back pore pressures of 300 to 400 kPa were used and the specimens were sheared at a strain rate of 5.5% per hour to allow the pore pressure to equilibrate throughout the soil during shearing. Most specimens exhibited strain strengthening characteristics except a few block samples which showed a peak deviatoric stress during shearing. The tests indicated an effective friction angle of 27 degrees and an effective cohesion of 20 kPa.

CONSTRUCTION AND GEOGRID LAYOUT

The site and foundation preparation were started on June 8, 1986 with grading of the site to a foundation elevation of 702 m. The foundation instrumentation was then installed to establish the zero reference values prior to fill construction. Placement of the embankment began on September 4, 1986 (day 0). The embankment reached a height of 3 m on October 23, 1986, when construction stopped due to the onset of freezing temperatures. The bottom primary reinforcement geogrid layer was placed 1 m above the ground surface during the first construction season. In 1987 rainy weather delayed placement of fill until August 30, 1987. An additional 3 m of fill was placed and the middle and the top layer of primary reinforcement geogrids, 3 and 5 m above the ground surface, were installed prior to construction shutdown on November 3, 1987. The test fill construction was resumed on August 10, 1988 and the 12 m designed fill height was completed on October 29, 1988. Figure 8 shows the fill height versus time throughout this extended construction period.

Three types of geogrids with different physical and mechanical properties were used in the test fill; Paragrid (50S/50S and 5T), Signode (TNX5001 and TNX250) and Tensar (SR2, SR1 and SS1). Each geogrid type reinforces one section of the test embankment (Fig. 2). The geogrids used in each section have two distinct roles. The primary geogrids were installed to reinforce against a deep seated failure within the slope. The secondary geogrids were to reinforce against shallow slope failures and to provide additional reinforcement against edge failure of the steep soil slope during the construction process from the construction equipment.

The primary geogrids were up to 13 meters long and were vertically spaced at 2 m to ensure that each geogrid acts independently within the soil mass. To guard against any possibility of pull out each geogrid was embedded in the embankment at least 4 m beyond the predicted critical slip surface. The secondary geogrids had lengths varying between 3 and 5 m and were spaced 1 m vertically. Figure 3 shows the cross-section of the embankment with the geogrid layout.

INSTRUMENTATION

Extensive instrumentation was installed to measure the performance of the foundation, the fill soil and the geogrids. The main goal of the instruments is to indicate the overall deformation of the fill and the foundation soils, the interaction between soil and geogrids, and pore pressure response

throughout the test fill during and subsequent to the construction. The layout of the soil and geogrid instrumentation is shown in Figures 9 and 10.

The strain in the geogrids were monitored using Bison strain gauges and electrical wire resistance strain gauges (EWR). Figure 10 shows the instrumented positions starting at 0.5 m and then at 1 m intervals from the slope surface beyond the 1 m location. Pairs of Bison strain gauges were attached by plastic bolts placed through the center of adjacent transverse members in the geogrids. These gauges monitor the displacement between the two sensors and can measure strains beyond the range of strain at which the electric wire resistance strain gauges would fail. Dummy Bison gauges were installed to check and correct some uncertain variations such as readout box sensitivity and temperature change. A pair of EWR strain gauges were installed at each instrumented position on the top and the bottom of a longitudinal member of the geogrid to measure the small strain induced in the geogrid. Each gauge was bonded to the geogrid using epoxy and then waterproofed. A thermocouple was placed at each instrumented position to account for the influence of temperature. Dummy EWR strain gauges were also installed in the test fill at 0.5, 1 and 5 m from the slope surface to aid in accounting for the effect of temperature. The global strain recorded by the Bison gauges along with the local strain from EWR gauges were used to evaluate the stresses and the loads induced in the geogrids as the embankment deformed.

Movements of the soil in the fill and the foundation were monitored using extensometers and inclinometers, installed both horizontally and vertically in the fill and the foundation soils. The combination of measurements from these instruments gives the soil movements during and after construction.

Horizontal extensometers and inclinometers were placed at levels 0, 2, 4 and 6 m above the ground surface. The multipoint magnetic horizontal extensometers measured the horizontal displacement of the soil between adjacent magnets approximately two meters apart; the horizontal Sinco telescoping inclinometers measured vertical deflection every 0.6 m from one side of the test embankment to the other. Unfortunately, all instruments at the 6 m level were damaged shortly after their installation during the 1988 construction season.

Vertical extensometers and inclinometers were installed beneath the toe and the crest of the slope at each section of the test fill. The vertical extensometers measured settlement in the fill and the foundation soils. The deepest extensometer magnet was placed at the bottom of each access tube, 12 m below the ground surface in the stiff till, to serve as a datum. The vertical inclinometers measured horizontal movement of the fill and the foundation soils, in directions parallel and normal to the slope. No field readings were available from the vertical instruments beneath the crest of the slopes in all four sections of the test fill after the 1988 construction season due to unrepairable damage.

The pore pressure response of the fill soil and the foundation during construction and during the subsequent consolidation period was monitored using pneumatic piezometers. A total of 56 Sinco pneumatic piezometers were installed within the fill and the foundation soils at the four sections of the test fill.

FIELD MEASUREMENTS

STRAIN IN THE TENSAR PRIMARY GEOGRIDS

The field strain measurements from the two types of gauges provided strain distribution along the geogrids. The magnitudes of the measured strain from the two types of instrumentation were close to each other. Profiles of the strain distribution, measured by the EWR gauges at the end of the 1988 construction season in the three primary reinforcing layers of the Tensar geogrids are illustrated in Figure 11. The profiles show strain increasing from the slope surface into the fill,

reaching a maximum and decreasing with distance into the fill. The locations and the magnitudes of the peak strains varied from one profile to other, indicating the development of a shear zone within the reinforced soil and the mobilization of the tensile strength along the geogrids. Figure 12 shows the strain variation with time at typical locations along the top geogrid layer. The plots show the field measurements are consistent and the development of the strain within the geogrid is directly related to the construction of the fill (Figures 8 and 11).

HORIZONTAL MOVEMENT OF THE FILL

The horizontal movements of the fill at different levels were monitored using horizontal extensometers. The measured relative horizontal displacement between a target magnet and the reference magnet installed at the center of the fill at each level was interpreted to give the average horizontal strain of the soil between adjacent magnets approximately 2 m apart. Figure 13 illustrates the strain profiles, at the end of construction, at levels 0, 2 and 4 m above the ground surface. The profiles show the development of compression and extension within the soil at the ground level, and the variation and localization of the movement within the reinforced soil. The correspondence of the soil movement at three different levels with respect to the strain development in the three layers of the geogrids is also shown.

Horizontal movements of the foundation soils were monitored using vertical inclinometers. The biaxial vertical inclinometer measures the horizontal deformation parallel and perpendicular to the slope. Figure 14 illustrates profiles of the horizontal deflection, at different stages of construction and consolidation, at the toe of the fill normal to the slope. The deflections along the slope showed the same distribution but much smaller magnitudes.

VERTICAL MOVEMENT OF SOILS

Vertical movements of the fill and the foundation soils were monitored using a horizontal inclinometer, a vertical extensometer and by ground elevation survey. The horizontal inclinometer measured the relative vertical deflection of the casing installed at each level during the construction; the vertical extensometer and ground elevation survey measured absolute vertical movement at specific points within the embankment. Figure 15 shows the settlement profile measured six months after the completion of the fill. Each profile represents the overall settlement below the measuring level since the installation. The profiles show both the amount of soil deformation and indicate where the movements are localized. This information is necessary for the understanding of the deformation mechanism and failure modes of a reinforced slope.

PORE PRESSURES

Figure 16 illustrates the pore pressures measured using the piezometers installed in the fill soil. The pore pressure variation is directly related to the construction of the test fill shown in Figure 8. Pore pressures increased during fill placement and dissipated during the winters and after completion of the fill. The dissipation rate during the first winter was higher than in the subsequent periods. At the same elevation, higher pore pressure developed at locations close to the center of the fill during construction. The pore pressures at different locations tended to equilibrate during a consolidation period as pore water migrated within the fill.

CONCLUSIONS

An instrumented full scale test fill can play an important role in research on slopes reinforced with geogrids and geotextiles. Measurements from the Devon geogrid test fill is providing information for a better understanding of mechanism, deformation patterns and failure modes of geogrid reinforced cohesive soil slopes. An improved understanding will result in valuable guidance for more efficient and economical design of future geogrid reinforced slopes.

ACKNOWLEDGEMENTS

Alberta Transportation and Utilities funded this research project. The assistance of colleagues at the University of Alberta, and within the Geotechnical Section and Research and Development Branch and District 7 of Alberta Transportation and Utilities is greatly appreciated.

REFERENCES

Bassett, R.H. and Yeo, K.C., 1988. The Behavior of A Reinforced Trial Embankment on Soft Shallow Foundation. Proceedings of The International Geotechnical Symposium on Theory and Practice of Earth Reinforcement. Fukuoka Kyushu, Japan, pp. 371-376.

Chalaturnyk, R.J., 1988. The Behavior of A Reinforced Soil Slope. M. Sc. Thesis, Department of Civil Engineering, University of Alberta, Edmonton, Alberta, Spring, 320p.

Duncan, J.M., Low, B.K., and Schaefer, V.R., 1985. STABGM: A Computer Program for Slope Stability Analysis of Reinforced Embankments and Slopes. Virginia Polytechnical Institute and State University, Blacksburg, 28p.

Fannin,R.J. and Hermann, S., 1988. Field Behavior of Two Instrumented Reinforced Soil Slopes. Proceedings of The International Geotechnical Symposium on Theory and Practice of Earth Reinforcement. Fukuoka Kyushu, Japan, pp.277-282.

Hofmann, B.A., 1989. Evaluation of Soil Properties of The Devon Test Fill. M. Sc. Thesis, Department of Civil Engineering, University of Alberta, Edmonton, Alberta, Spring, 325p.

Jewell, R.A., Paine, N., and Woods, R.I., 1984. Design Method for Steep Reinforced Embankments. Proceedings of A Conference on Polymer Grid Reinforcement. Thomas Telford, London, pp. 70-81.

Murray, R., 1982. Fabric Reinforcement of Embankment and Cuttings. Proceedings of 2'nd International Conference on Geotextiles, Las Vegas, Vol. 3, pp. 695-701.

Rimoldi, P., 1988. A Review of Field Measurements of The Behavior of Geogrid Reinforced Slopes and Walls. Proceedings of The International Geotechnical Symposium on Theory and Practice of Earth Reinforcement. Fukuoka Kyushu, Japan, pp. 571-576.

Rowe, K., 1984. Reinforced Embankment: Analysis and Design. Journal of Geotechnical Engineering, ASCE, Vol. 110, pp. 231-246.

Schmertmann, G.R., Chouery-Curtis, V.E., Johnson, R.D., and Bouaparte, R., 1987. Design Charts for Geogrid-Reinforced Soil Slopes. Conference Proceedings of Geosynthetics'87, New Orleans, pp. 108-120.

Sego, D.C., Scott, J.D., Richards, E.A., and Liu, Y., 1990. Performance of A Geogrid in A Cohesive Soil Test Embankment. 4th International Conference on Geotextiles, Geomembranes and Related Products. The Hague, Netherlands, pp. 67-72.

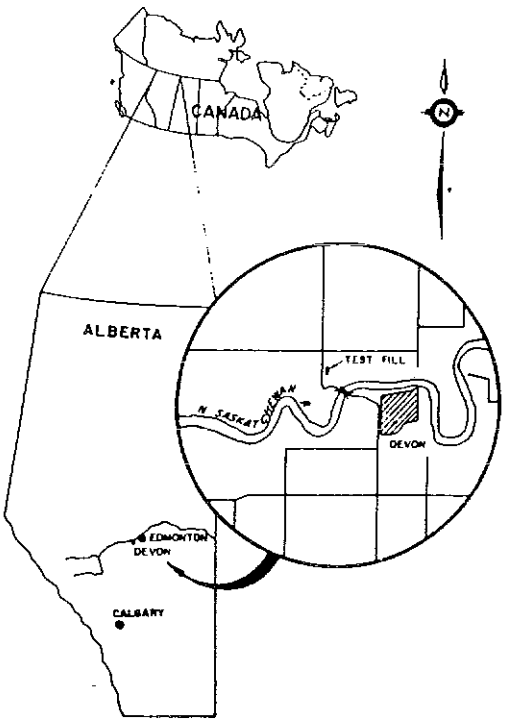

Figure 1. Location of Devon Test Fill

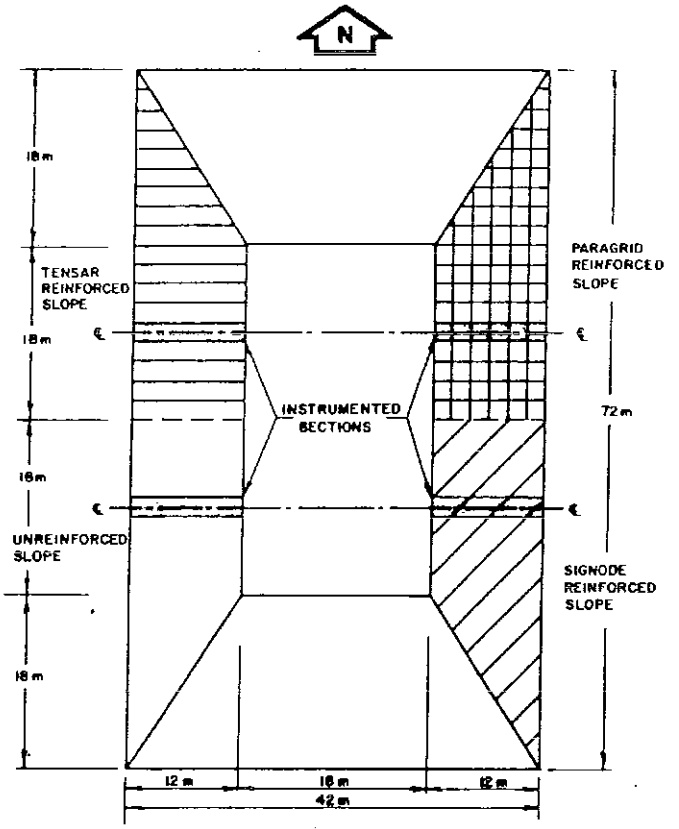

Figure 2. Plan view of test fill

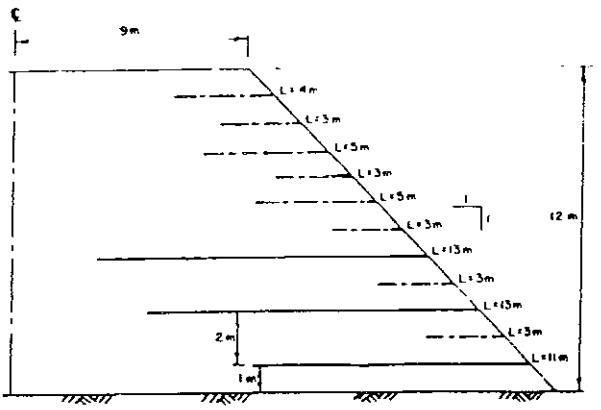

Figure 3. Geogrid layout in test fill

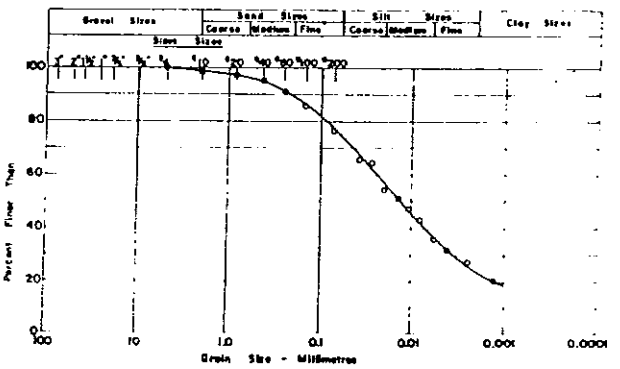

Figure 4. Grain size curve of fill soil

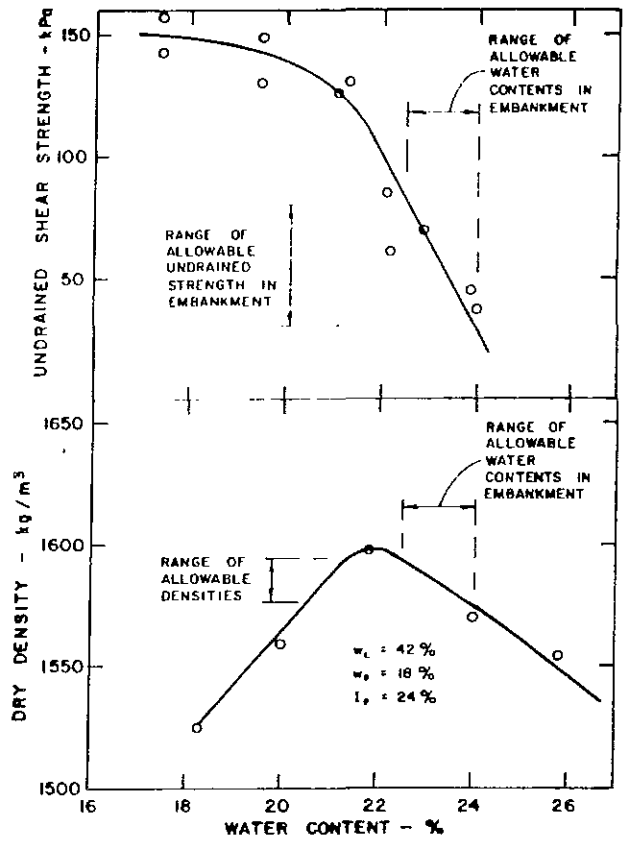

Figure 5. Results of compaction test of fill soil

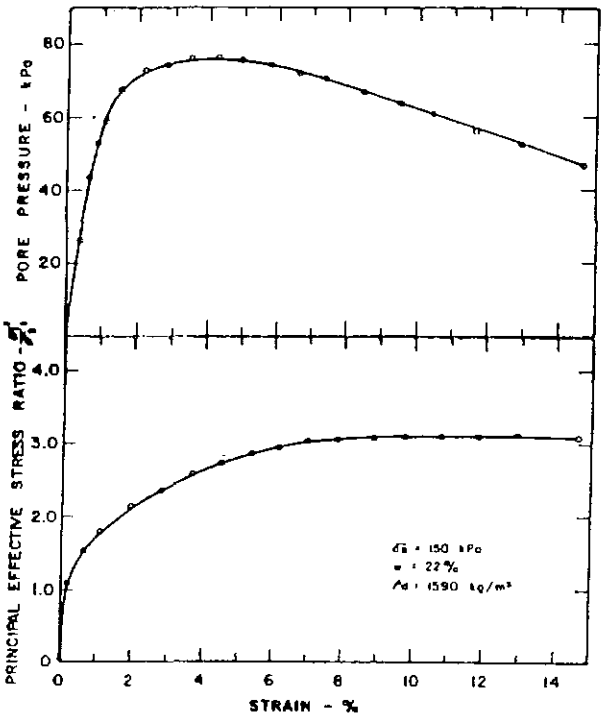

Figure 6. Stress strain properties and pore pressure response of fill soil

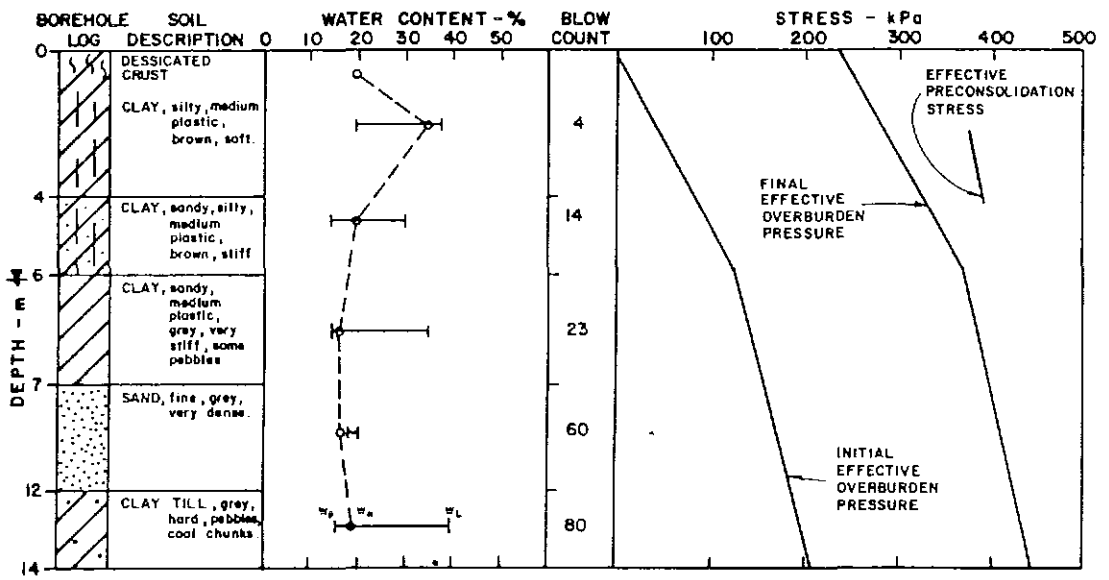

Figure 7. Foundation soil profile

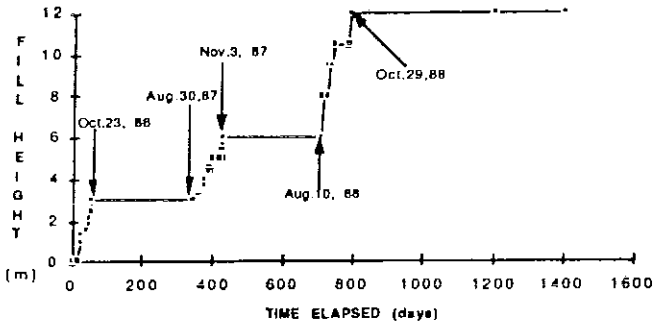

Figure 8. Construction schedule of test fill

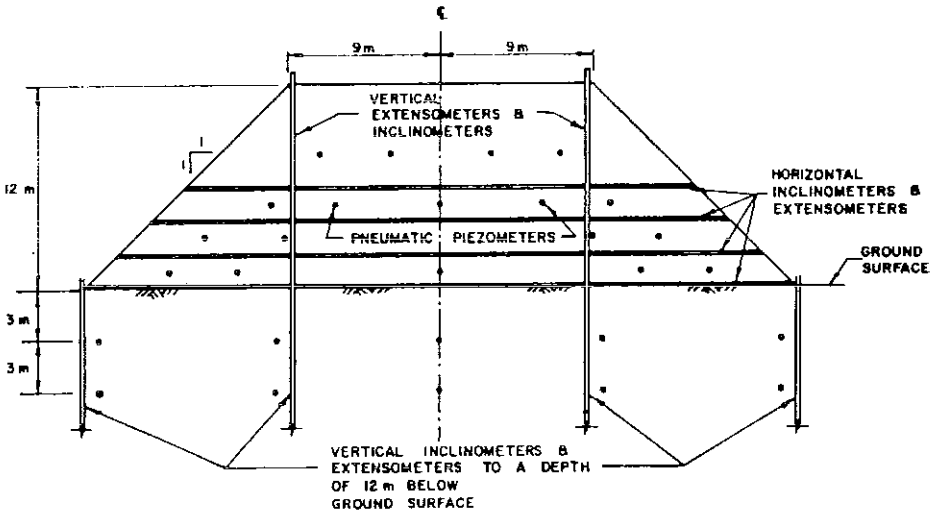

Figure 9. Layout of soil instrumentation in test fill

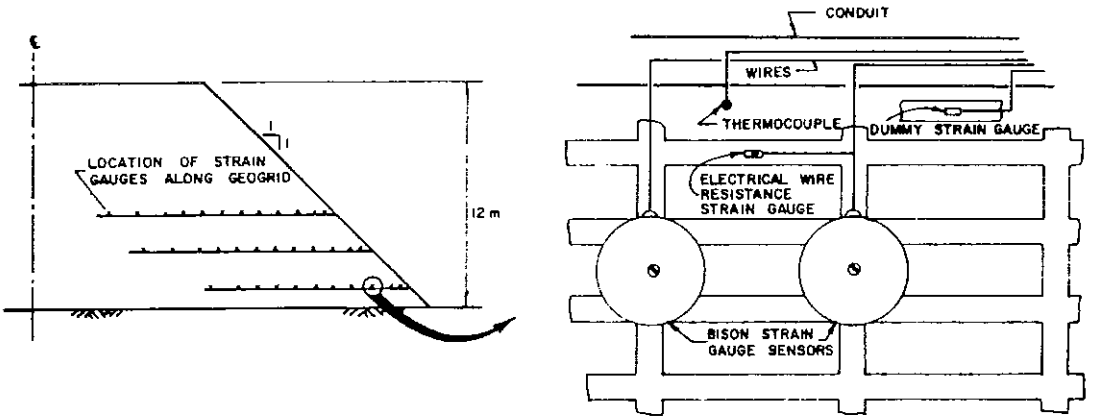

Figure 10. Instrumented position in geogrids

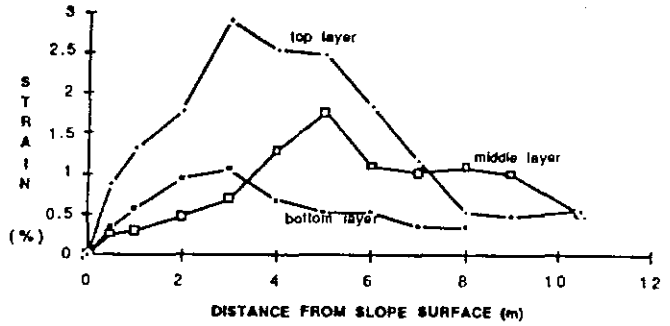

Figure 11. Tensile strain distribution in Tensar geogrid

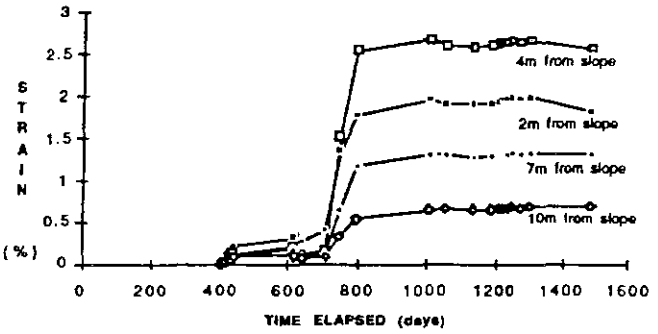

Figure 12. Development of tensile strain in Tensar geogrid

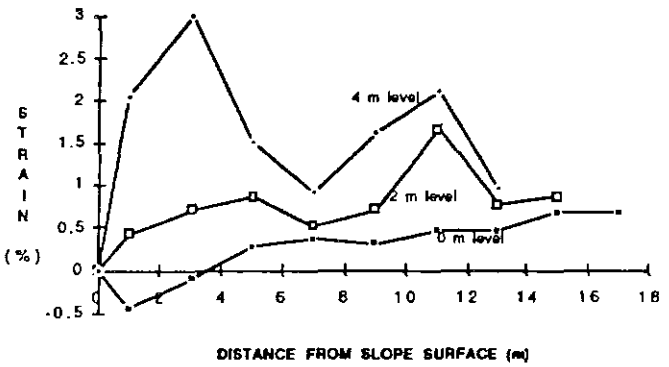

Figure 13. Horizontal strain distribution of soil in Tensar section

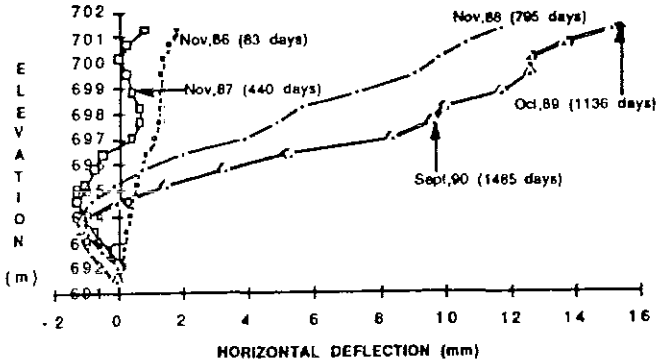

Figure 14. Horizontal deflection of foundation soils in Tensar section

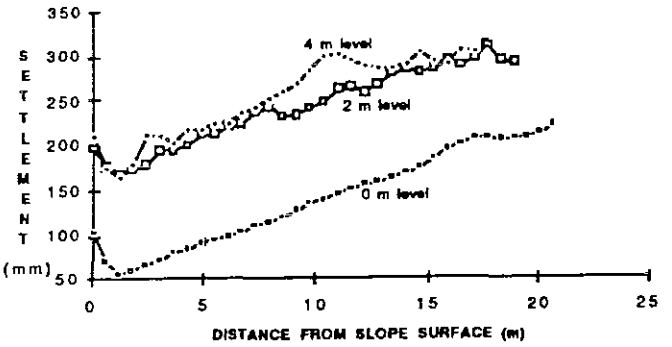

Figure 15. Settlement profiles in Tensar section

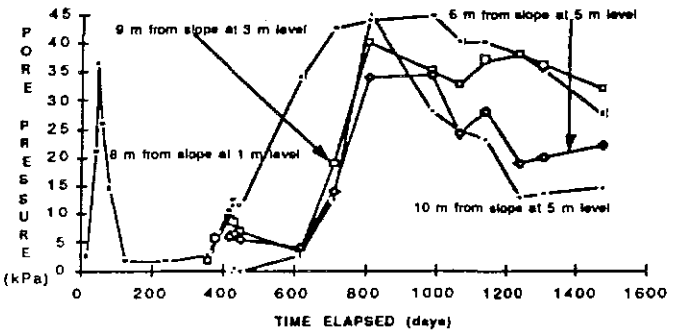

Figure 16. Pore pressure response of fill soil in Tensar section